

Chapter 2

Lattice Vibrations and Heat Capacity

Einstein's and Debye's theories of the heat capacity of a solid are presented. The quantum particles (phonons) for the lattice vibrations are introduced.

2.1 Einstein's Theory of Heat Capacity

Let us consider a crystal lattice at low temperatures. We may expect each atom forming the lattice to execute small oscillations around the equilibrium position. For illustration let us consider the one-dimensional lattice shown in Figure 2.1. The motion of the j th atom may be characterized by the Hamiltonian of the form:

$$h_j = \frac{p_j^2}{2M} + \frac{1}{2}k_0u_j^2, \quad (2.1)$$

where u_j denotes displacement and $p_j = M\dot{u}_j$ represents the momentum. Here we assumed a parabolic potential, which is reasonable for small oscillations. If the *equipartition theorem* is applied, the kinetic and potential energy parts each contribute $k_B T/2$ to the average thermal energy. We then obtain

$$\langle h \rangle = \left\langle \frac{1}{2M}p^2 \right\rangle + \left\langle \frac{1}{2}k_0u^2 \right\rangle = \frac{1}{2}k_B T + \frac{1}{2}k_B T = k_B T. \quad (2.2)$$

Multiplying Equation (2.2) by the number of atoms N , we obtain $Nk_B T$ for the total energy. By differentiating it with respect to T , we obtain the heat capacity Nk_B for the lattice.

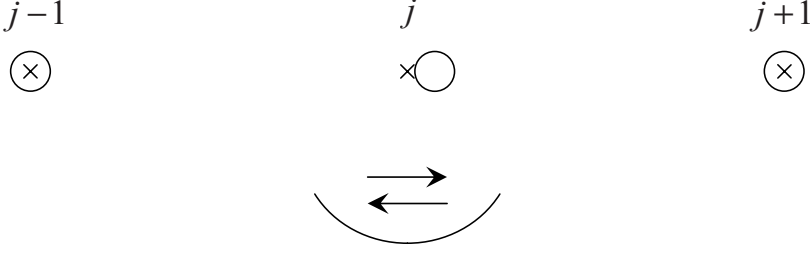


Figure 2.1: The j th atom in the linear chain executes simple harmonic oscillations as characterized by the Hamiltonian in Equation (2.1).

In quantum theory the eigenvalues of the Hamiltonian

$$h = \frac{p^2}{2M} + \frac{1}{2}k_0 u^2 \quad (2.3)$$

are given by

$$\epsilon_n = \left(\frac{1}{2} + n \right) \hbar \omega_0, \quad n = 0, 1, 2, \dots, \quad (2.4)$$

$$\omega_0 \equiv \left(\frac{k_0}{M} \right)^{1/2}. \quad (2.5)$$

The quantum states are characterized by nonnegative integers n . If we assume a canonical ensemble of simple harmonic oscillators with the distribution $\exp(-\beta\epsilon)$, the average energy can be calculated as follows:

$$\begin{aligned} \langle h \rangle &= \frac{\sum_n \epsilon_n e^{-\beta\epsilon_n}}{\sum_n e^{-\beta\epsilon_n}} = -\frac{\partial}{\partial\beta} \ln \left(\sum_n e^{-\beta\epsilon_n} \right) = -\frac{\partial}{\partial\beta} \ln \left(\sum_{n=0}^{\infty} e^{-\beta(1/2+n)\hbar\omega_0} \right) \\ &= -\frac{\partial}{\partial\beta} \ln \left(\frac{e^{-\beta\hbar\omega_0/2}}{1 - e^{-\beta\hbar\omega_0}} \right) = \left[\frac{1}{2} + f_0(\hbar\omega_0) \right] \hbar\omega_0, \end{aligned} \quad (2.6)$$

$$f_0(\eta) \equiv \frac{1}{e^{\beta\eta} - 1}. \quad (2.7)$$

Here f_0 represents the *Planck distribution function*. Notice that the quantum average energy $\langle h \rangle$ in Equation (2.6) is quite different from the classical average energy $k_B T$ [see Equation (2.2)].

Let us now consider N atoms in a three-dimensional lattice. We multiply Equation (2.6) by the number of degrees of freedom, $3N$ and obtain for the total energy

$$E = 3N \left[\frac{1}{2} + f_0(\hbar\omega_0) \right] \hbar\omega_0. \quad (2.8)$$

Differentiating this with respect to T , we obtain the heat capacity at constant volume C_V (Problem 2.1.1):

$$C_V = \frac{\partial E}{\partial T} = \frac{\partial E}{\partial \beta} \frac{\partial \beta}{\partial T} = \frac{3N(\hbar\omega_0)^2}{k_B T^2} \frac{e^{\beta\hbar\omega_0}}{(e^{\beta\hbar\omega_0} - 1)^2}.$$

We rewrite this expression in the form (Problem 2.1.1)

$$C_V = 3Nk_B \left(\frac{\Theta_E}{T} \right)^2 e^{\Theta_E/T} (e^{\Theta_E/T} - 1)^{-2}, \quad (2.9)$$

where

$$\Theta_E \equiv \frac{\hbar\omega_0}{k_B} = \left(\frac{\hbar}{k_B} \right) \left(\frac{k_0}{M} \right)^{1/2} \quad (2.10)$$

is the *Einstein temperature*. The function

$$g(x) \equiv x^2 e^x (e^x - 1)^{-2} \quad \left(x \equiv \frac{\Theta_E}{T} \right) \quad (2.11)$$

has the asymptotic behavior (Problem 2.1.2)

$$g(x) \approx \begin{cases} x^2 e^{-x} & \text{for } x \gg 1 \\ 1 & \text{for } x \ll 1. \end{cases} \quad (2.12)$$

At very high temperatures ($\Theta_E/T \ll 1$), the heat capacity given by Equation (2.9) approaches the classical value $3Nk_B$:

$$C_V = 3Nk_B g \left(\frac{\Theta_E}{T} \right) \longrightarrow 3Nk_B. \quad (2.13)$$

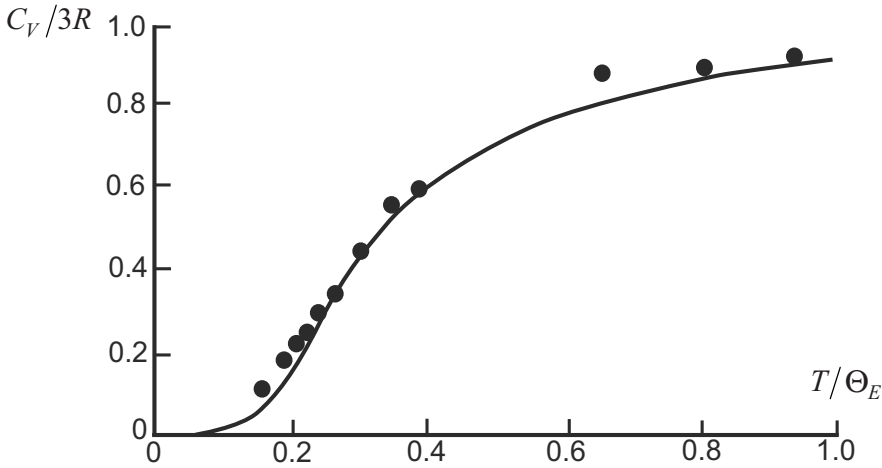


Figure 2.2: The molar heat capacity for Einstein's model of a solid is shown in a solid line. Experimental points are for a diamond with $\Theta_E = 1320$ K.

At very low temperatures ($\Theta_E/T \gg 1$), the heat capacity C_V behaves like

$$C_V \approx 3Nk_B \left(\frac{\Theta_E}{T} \right)^2 \exp \left(\frac{-\Theta_E}{T} \right) \quad (2.14)$$

and approaches zero exponentially as T tends to zero. The behavior of $C_V/3Nk_B$ from Equation (2.9) is plotted against Θ_E/T in Figure 2.2. Experimental data of C_V for diamond are shown by points with the choice of $\Theta_E = 1320$ K for comparison. The fit is quite reasonable for diamond. Historically Einstein [1] obtained Equation (2.9) in 1907 before the advent of quantum theory in 1925–26. The discrepancy between experiment and theory (equipartition theorem) had been a mystery until 1907.

Problem 2.1.1. Derive Equation (2.9), using Equations (2.7) and (2.8).

Problem 2.1.2. Verify the asymptotic behavior of Equation (2.12) from Equation (2.11).

2.2 Debye's Theory of Heat Capacity

In Section 2.1, we discussed Einstein's theory of the heat capacity of a solid. This theory explains why a certain solid like a diamond exhibits a molar heat capacity substantially smaller than $3R$. It also predicts that the heat capacity for any solid should decrease as the temperature is lowered. This prediction is in agreement with experimental observations. However, the temperature dependence at very low temperatures indicates nonnegligible discrepancies. In 1912 Debye [2] reported a very successful theory of the heat capacity of solids, which will be discussed in this section.

In Einstein's model the solid is viewed as a collection of free harmonic oscillators with a *common* frequency ω_0 . This is rather a drastic approximation, because an atom in a real crystal moves under the varying potential field generated by its neighboring atoms. It is more reasonable to look at the crystal as a collection of *coupled* harmonic oscillators. The motion of a set of coupled harmonic oscillators can be described concisely in terms of the normal modes of oscillations. A major difficulty of this approach, however, is to find the set of the normal-mode frequencies. Debye overcame this difficulty by regarding a solid as a *continuous elastic body* whose normal modes of oscillations are known as *elastic waves*. We note that this is valid only at low frequencies.

A macroscopic solid can support transverse and longitudinal waves. We first look at the case of the transverse wave. The equation of motion for the transverse elastic wave is

$$\rho \frac{\partial^2 \mathbf{u}}{\partial t^2} = S \nabla^2 \mathbf{u}, \quad (2.15)$$

where \mathbf{u} is the transverse displacement lying in a plane perpendicular to the direction of the wave propagation, ρ is the mass density, and S the shear modulus. Since the displacement (component) u_j is a continuous-field (opposed to a discrete) variable, the usual Lagrangian formulation does not work. However its generalization is immediate. We use a *Lagrangian field method* as follows.

We introduce a Lagrangian density \mathcal{L} , which is a function of the displacement components, their time-derivatives, and space-derivatives:

$$\mathcal{L} = \mathcal{L} \left(u_x, u_y, u_z, \frac{\partial u_x}{\partial t}, \frac{\partial u_y}{\partial t}, \frac{\partial u_z}{\partial t}, \frac{\partial u_x}{\partial x}, \dots \right). \quad (2.16)$$

We then derive the equations of motion by means of *Lagrange's field equations*:

$$\begin{aligned} \frac{\partial}{\partial t} \left(\frac{\partial \mathcal{L}}{\partial (\partial u_a / \partial t)} \right) + \frac{\partial}{\partial x} \left(\frac{\partial \mathcal{L}}{\partial (\partial u_a / \partial x)} \right) + \frac{\partial}{\partial y} \left(\frac{\partial \mathcal{L}}{\partial (\partial u_a / \partial y)} \right) \\ + \frac{\partial}{\partial z} \left(\frac{\partial \mathcal{L}}{\partial (\partial u_a / \partial z)} \right) - \frac{\partial \mathcal{L}}{\partial u_a} = 0, \quad a = x, y, z. \end{aligned} \quad (2.17)$$

In our case we may choose

$$\mathcal{L} = \frac{1}{2} \rho \left| \frac{\partial \mathbf{u}}{\partial t} \right|^2 - \frac{1}{2} S \left(\left| \frac{\partial \mathbf{u}}{\partial x} \right|^2 + \left| \frac{\partial \mathbf{u}}{\partial y} \right|^2 + \left| \frac{\partial \mathbf{u}}{\partial z} \right|^2 \right) \quad (2.18)$$

$$= \frac{1}{2} \rho \left[\left(\frac{\partial u_x}{\partial t} \right)^2 + \left(\frac{\partial u_y}{\partial t} \right)^2 + \left(\frac{\partial u_z}{\partial t} \right)^2 \right] - \dots, \quad (2.19)$$

and verify the correct equation of motion (2.15) by using Equations (2.17) and (2.19) (Problem 2.2.1).

Let us assume a cubic box (with the side length L_0) fixed-end boundary condition. The normal modes of oscillations are represented by the amplitude functions

$$\sin(xk_x) \sin(yk_y) \sin(zk_z), \quad (2.20)$$

$$k_a \equiv \frac{\pi n_a}{L_0}, \quad n_a = 1, 2, \dots, \quad a = x, y, z, \quad (2.21)$$

and the angular frequencies

$$\omega_{t,k} = c_t |\mathbf{k}| = \left(\frac{S}{\rho} \right)^{1/2} k, \quad (2.22)$$

where c_t is the speed of propagation for the transverse (t) wave. The wave vector \mathbf{k} is perpendicular to the displacement \mathbf{u} :

$$\mathbf{k} \cdot \mathbf{u} = 0 \quad (\text{transverse wave}). \quad (2.23)$$

We now wish to express the Lagrangian density \mathcal{L} in terms of the normal coordinates and velocities. Let us denote the Cartesian components of \mathbf{u} by u_1 and u_2 . We introduce the *normal coordinates*:

$$q_{\mathbf{k},\sigma}(t) = \left(\frac{2}{L_0} \right)^3 \int_0^{L_0} dx \int_0^{L_0} dy \int_0^{L_0} dz u_\sigma \sin(xk_x) \sin(yk_y) \sin(zk_z), \quad (2.24)$$

where $\sigma = 1, 2$ are called the *polarization indices*. After lengthy but straightforward calculations, we can then transform the Lagrangian density \mathcal{L} into (Problem 2.2.2)

$$\mathcal{L} = \sum_{\mathbf{k}} \sum_{\sigma} \left(\frac{1}{4} \rho \dot{q}_{\mathbf{k},\sigma}^2 - \frac{1}{4} S k^2 q_{\mathbf{k},\sigma}^2 \right), \quad (2.25)$$

which is the sum of single-mode Lagrangian densities: $(1/4)\rho\dot{q}_{\mathbf{k},\sigma}^2 - (1/4)Sk^2q_{\mathbf{k},\sigma}^2$.

The Lagrangian L is the Lagrangian density \mathcal{L} times the volume V :

$$L \equiv V\mathcal{L}. \quad (2.26)$$

For later convenience we introduce new normal coordinates:

$$Q_{\mathbf{k},\sigma} \equiv \left(\frac{V\rho}{2} \right)^{1/2} q_{\mathbf{k},\sigma}. \quad (2.27)$$

By using these coordinates, we can re-express the Lagrangian L as follows:

$$L = \sum_{\mathbf{k}} \sum_{\sigma} \frac{1}{2} \left[\dot{Q}_{\mathbf{k},\sigma}^2 - \omega_{t,k}^2 Q_{\mathbf{k},\sigma}^2 \right]. \quad (2.28)$$

To derive the corresponding Hamiltonian, we define the *canonical momenta* $\{P_{\mathbf{k},\sigma}\}$ by

$$P_{\mathbf{k},\sigma} \equiv \frac{\partial L}{\partial \dot{Q}_{\mathbf{k},\sigma}} = \dot{Q}_{\mathbf{k},\sigma}. \quad (2.29)$$

The Hamiltonian H_t for the transverse waves can then be constructed by expressing $\sum_{\mathbf{k}} \sum_{\sigma} P_{\mathbf{k},\sigma} \dot{Q}_{\mathbf{k},\sigma} - L$ in terms of $\{Q_{\mathbf{k},\sigma}, P_{\mathbf{k},\sigma}\}$. The result is given by

$$H_t = \sum_{\mathbf{k}} \sum_{\sigma} \frac{1}{2} \left[P_{\mathbf{k},\sigma}^2 + \omega_{t,k}^2 Q_{\mathbf{k},\sigma}^2 \right]. \quad (2.30)$$

The normal modes of oscillations characterized by k -vector \mathbf{k} , polarization σ , and frequency $\omega_{t,k}$ represent *standing waves*, which arise from the fixed-end boundary condition. If we assume a periodic box boundary condition, the normal modes are the *running waves*. In either case the results for the heat capacity are the same.

The energy eigenvalues for the corresponding quantum Hamiltonian for the system are

$$E_t = \sum_{\mathbf{k}} \sum_{\sigma} \left(\frac{1}{2} + n_{\mathbf{k},\sigma} \right) \hbar \omega_{t,k} = E[\{n_{\mathbf{k},\sigma}\}], \quad (2.31)$$

$$n_{\mathbf{k},\sigma} = 0, 1, 2, \dots \quad (2.32)$$

It is convenient to interpret Equation (2.31) in terms of the energies of quantum particles called *phonons*. In this view the quantum number $n_{\mathbf{k},\sigma}$ represents the number of phonons in the normal mode (\mathbf{k}, σ) . The energy of the system is then specified by the set of the numbers of phonons in normal modes (states), $\{n_{\mathbf{k},\sigma}\}$.

By taking the canonical ensemble average of Equation (2.31), we obtain

$$\begin{aligned} \langle E_t \rangle &= \sum_{\mathbf{k}} \sum_{\sigma} \left(\frac{1}{2} + \langle n_{\mathbf{k},\sigma} \rangle \right) \hbar \omega_{t,k} \\ &= \sum_{\mathbf{k}} \sum_{\sigma} \left[\frac{1}{2} + f_0(\hbar \omega_{t,k}) \right] \hbar \omega_{t,k} \equiv E_t(\beta), \end{aligned} \quad (2.33)$$

$$\langle n_{\mathbf{k},\sigma} \rangle = \frac{1}{e^{\beta \epsilon} - 1} \equiv f_0(\epsilon). \quad (2.34)$$

When the volume of normalization V is made large, the distribution of the normal-mode points in the k -space becomes dense. In the bulk limit we may convert the sum over $\{\mathbf{k}\}$ in Equation (2.33) into an ω -integral and obtain

$$E_t(\beta) = E_{t,0} + \int_0^\infty d\omega \hbar \omega f_0(\hbar \omega) \mathcal{D}_t(\omega), \quad (2.35)$$

$$E_{t,0} \equiv \frac{1}{2} \int_0^\infty d\omega \hbar \omega \mathcal{D}_t(\omega), \quad (2.36)$$

where $\mathcal{D}_t(\omega)$ is the *density of states (modes) in the frequency domain* defined such that

$$\text{Number of modes in the interval } (\omega, \omega + d\omega) \equiv \mathcal{D}_t d\omega, \quad (2.37)$$

and $E_{t,0}$ represents the sum of zero-point energies, which is independent of temperature.

The density of states in the frequency domain $\mathcal{D}_t(\omega)$ may be calculated as follows. First we note that the angular frequency ω is related to the wave vector \mathbf{k} by $\omega = c_t k$. The constant- ω surface in the k -space is therefore the sphere of radius $k = \omega/c_t$. Consider another concentric sphere of radius $k + dk = (\omega + d\omega)/c_t$. Each mode point is located at the SC lattice sites with unit spacing π/L_0 and only in the first octant ($k_x, k_y, k_z > 0$). The number of mode points within the spherical shell between the two spheres can be obtained by dividing one-eighth of the k -volume of the shell:

$$\frac{(4\pi k^2 dk)}{8} = \left(\frac{1}{2}\right) \frac{\pi \omega^2 d\omega}{c_t^3} \quad (\omega = c_t k)$$

by the unit-cell k -volume, $(\pi/L_0)^3$. Multiplying the result by 2 in consideration of the polarization multiplicity, we obtain

$$\mathcal{D}_t(\omega) d\omega = \frac{\pi(\omega^2 d\omega/c_t^3)}{(\pi/L_0)^3} = \frac{L_0^3 \omega^2 d\omega}{\pi^2 c_t^3} = \frac{V \omega^2 d\omega}{\pi^2 c_t^3}. \quad (2.38)$$

We may treat the longitudinal waves similarly. The average energy $E_l(\beta) \equiv \langle E_l[\{n_{\mathbf{k}}\}] \rangle$ can be written in the same form as Equation (2.33) with the density of states

$$\mathcal{D}_l(\omega) = \frac{V \omega^2}{2\pi^2 c_l^3}; \quad (2.39)$$

$$c_l \equiv \left[\frac{(B + 3S/4)}{\rho} \right]^{1/2} \quad (2.40)$$

is the propagation speed of the longitudinal wave; $B \equiv -V^{-1} \partial P / \partial V)_T$ is the bulk modulus. Combining the two wave modes together, we obtain

$$E \equiv E_t + E_l = E_0 + \int_0^\infty d\omega \hbar \omega f_0(\hbar \omega) \mathcal{D}(\omega), \quad (2.41)$$

$$E_0 \equiv \frac{1}{2} \int_0^\infty d\omega \hbar \omega \mathcal{D}(\omega), \quad (2.42)$$

where

$$\mathcal{D}(\omega) \equiv \mathcal{D}_t(\omega) + \mathcal{D}_l(\omega) = \frac{V}{2\pi^2} \left(\frac{2}{c_t^3} + \frac{1}{c_l^3} \right) \omega^2 \quad (2.43)$$

denotes the density of states in frequency for the combined wave modes.

For a real crystal of N atoms, the number of degrees of freedom is $3N$. Therefore, there exist exactly $3N$ normal modes. The elastic body whose dynamic state is described by the vector field $\mathbf{u}(\mathbf{r}, t)$ has an infinite number of degrees of freedom, and therefore, it has infinitely many modes. The model of a macroscopic elastic body is a reasonable representation of a real solid for low-frequency modes, that is, long-wavelength modes. At high frequencies the continuum model does not provide normal modes expected of a real solid. Debye solved the problem by assuming that the density of states $\mathcal{D}_D(\omega)$ has the same value as given by Equation (2.43) up to the maximum frequency ω_D , then vanishes thereafter,

$$\mathcal{D}_D(\omega) = \begin{cases} \frac{V}{2\pi^2} \left(\frac{2}{c_t^3} + \frac{1}{c_l^3} \right) \omega^2 & \omega < \omega_D \\ 0 & \text{otherwise,} \end{cases} \quad (2.44)$$

and that the limit frequency ω_D , called the *Debye frequency*, is chosen such that the number of modes for the truncated continuum model equals $3N$:

$$\int_0^\infty d\omega \mathcal{D}_D(\omega) = \int_0^{\omega_D} d\omega \mathcal{D}(\omega) = 3N. \quad (2.45)$$

Substitution of Equation (2.44) yields (Problem 2.2.3.)

$$\omega_D = \left[18\pi^2 n / \left(\frac{2}{c_t^3} + \frac{1}{c_l^3} \right) \right]^{1/3}, \quad (2.46)$$

where $n \equiv N/V$ is the number density. The density of states $\mathcal{D}_D(\omega)$ grows quadratically, reaches the maximum at $\omega = \omega_D$, then vanishes thereafter as shown in Figure 2.3.

We now compute the heat capacity C_V . Introducing Equation (2.44) into Equation (2.41), we obtain

$$\begin{aligned} E(T) - E_0 &= \int_0^{\omega_D} d\omega \hbar\omega f_0(\hbar\omega) \frac{V}{2\pi^2} \left(\frac{2}{c_t^3} + \frac{1}{c_l^3} \right) \omega^2 \\ &= \frac{9N\hbar}{\omega_D^3} \int_0^{\omega_D} d\omega \frac{\omega^3}{\exp(\hbar\omega/k_B T) - 1}. \end{aligned} \quad (2.47)$$

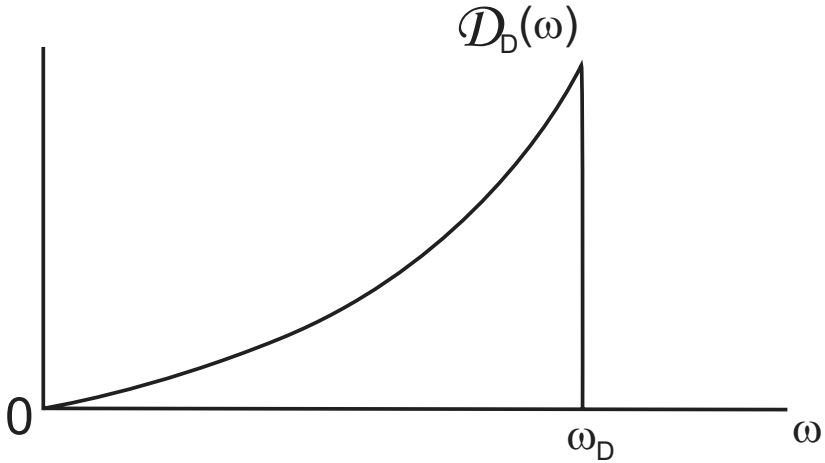


Figure 2.3: The density of modes in angular frequency for the Debye model.

Introducing the *Debye temperature* Θ_D defined by

$$\Theta_D \equiv \frac{\hbar \omega_D}{k_B}, \quad (2.48)$$

we can rewrite Equation (2.47) as

$$E(T) - E_0 = 9Nk_B T \left(\frac{T}{\Theta_D} \right)^3 \int_0^{x_D} dx \frac{x^3}{e^x - 1}, \quad (2.49)$$

$$x_D \equiv \frac{\hbar \omega_D}{k_B T} \equiv \frac{\Theta_D}{T}, \quad x \equiv \frac{\hbar \omega}{k_B T}. \quad (2.50)$$

Consider first the high-temperature region where $x \equiv \hbar \omega / k_B T \ll 1$. Then $e^x - 1 \approx x$ and

$$\int_0^{x_D} dx \frac{x^3}{e^x - 1} \simeq \int_0^{x_D} dx x^2 = \frac{x_D^3}{3} = \frac{1}{3} \left(\frac{\Theta_D}{T} \right)^3, \quad x_D \ll 1. \quad (2.51)$$

Using this approximation, we obtain from Equation (2.49)

$$E(T) = E_0 + 3Nk_B T, \quad T \gg \Theta_D. \quad (2.52)$$

Differentiating Equation (2.52) with respect to T , we obtain the heat capacity of the solid, $C_V = \partial E / \partial T = 3Nk_B$, which is in agreement with the Dulong–Petit’s law.

At very low temperatures, $x_D \equiv \hbar\omega_D/k_B T$ becomes very large. In the limit, we have

$$\begin{aligned} \int_0^{\omega_D} dx \frac{x^3}{e^x - 1} &\longrightarrow \int_0^\infty dx \frac{x^3}{e^x - 1} \\ &= \int_0^\infty dx x^3 e^{-x} (1 + e^{-x} + e^{-2x} + \cdots) \\ &= \sum_{n=1}^\infty \frac{6}{n^4} = \frac{\pi^4}{15}. \end{aligned} \quad (2.53)$$

We then obtain from Equation (2.49)

$$E = E_0 + \left(\frac{3}{5}\right) \frac{\pi^4 Nk_B T^4}{\Theta_D^3} \quad (T \ll \Theta_D). \quad (2.54)$$

Differentiating this expression with respect to T , we obtain

$$\boxed{C_V = \frac{12\pi^2}{5} Nk_B \left(\frac{T}{\Theta_D}\right)^3.} \quad (2.55)$$

According to this equation, the heat capacity at very low temperatures behaves like T^3 . This is known as the *Debye T^3 law*. The decrease is therefore slower than the Einstein heat capacity given by Equation (2.14), which decreases exponentially.

At intermediate temperatures the integral may be evaluated as follows. Differentiating Equation (2.47) with respect to T , we obtain

$$\boxed{C_V = 9Nk_B \left(\frac{T}{\Theta_D}\right)^3 \int_0^{x_D} dx \frac{x^4 e^x}{(e^x - 1)^2} \quad \left(x_D \equiv \frac{\Theta_D}{T}\right).} \quad (2.56)$$

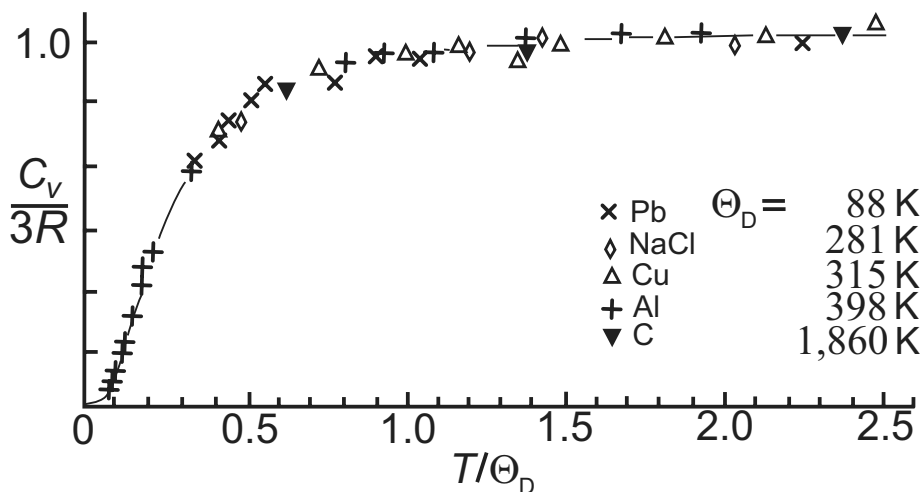


Figure 2.4: The heat capacities of solids. The solid line represents the Debye curve obtained from Equation (2.55). Experimental data for various solids are shown with optimum Debye temperatures, after Sears and Salinger [3].

We can compute this integral numerically. We then express the molar heat of solid as a function of T/Θ_D only. The theoretical curve obtained is shown in a solid line in Figure 2.4. The points in the figure are experimental data for various solids. The Debye temperatures adjusted at optimum fitting are also shown in the same figure. Roughly speaking when T/Θ_D is greater than 1 or when the actual temperature exceeds the Debye temperature, the solid behaves classically, and the molar heat is nearly equal to $3R$ in agreement with the Dulong–Petit’s law. When the temperature is less than the Debye temperature, the quantum effect sets in; so the heat capacity is less than $3R$. Thus, for lead (a soft metal) with a Debye temperature of only 88 K, room temperature is well above the Debye temperature. Therefore, its heat capacity has a classical value. Diamond (a hard crystal) with a Debye temperature of 1860 K, shows a quantum nature in heat capacity even at room temperature. The Debye temperatures for several typical solids are given in Table 2.1.

Debye’s theory of the heat capacity gives quite satisfactory results for almost all nonconducting crystals. Exceptions arise if the crystals have striking

Table 2.1: Approximate Debye Temperature Values

Solids	Debye temperature Θ_D in K
NaCl	281
KCl	230
Pb	88
Ag	225
Zn	308
Diamond	1860

anisotropies like graphite or if finite-size crystals are considered. For conducting materials we must take into account the electronic contribution to the heat capacity, which will be discussed in Chapter 3. We may look at a solid as a collection of coupled harmonic oscillators and develop a theory from this viewpoint.

Problem 2.2.1. Verify Equation (2.15) by using Equations (2.17) and (2.19).

Problem 2.2.2. Verify Equation (2.25).

Problem 2.2.3. Verify Equation (2.46).

Quantum Theory of Conducting Matter

Newtonian Equations of Motion for a Bloch Electron

Fujita, S.; Ito, K.

2007, XX, 244 p. 80 illus.,

ISBN: 978-0-387-74103-1